NoLoRa: Ultra-Low-Power LoRa Transmissions Without Active Radios for Battery-Free Devices

Citation for published version:
Majumder, S, Birk, J, Lohr, C, Goussetis, G, Asimonis, SD & Daskalakis, S 2026, NoLoRa: Ultra-Low-Power LoRa Transmissions Without Active Radios for Battery-Free Devices. in *IEEE European Conference on Antennas and Propagation (EuCAP) 2026.* IEEE, 20th European Conference on Antennas and Propagation 2026, Dublin, Ireland, 19/04/26.

Link:
Link to publication record in Heriot-Watt Research Portal

Document Version:
Peer reviewed version

Published In:
IEEE European Conference on Antennas and Propagation (EuCAP) 2026

NoLoRa: Ultra-Low-Power LoRa Transmissions Without Active Radios for Battery-Free Devices

Shayan Majumder[1], Julian Birk[1], Charles Lohr[2], George Goussetis[1],
Stylianos D. Asimonis[3] and Spyridon N. Daskalakis[1]
[1]School of Engineering and Physical Sciences, Heriot-Watt University, Edinburgh EH14 4AS, Scotland, UK
{sm3054, jbb2002, g.goussetis, s.daskalakis}@hw.ac.uk
[2] Bellevue, Washington, United States
lohr85@gmail.com
[3] Department of Electrical and Computer Engineering, University of Patras, 26504 Patras, Greece
s.asimonis@upatras.gr

***Abstract*—This paper presents "NoLoRa," a novel method for achieving LoRaWAN-compatible communication without dedicated radio transceivers or batteries. The system leverages electromagnetic emissions from digital signals in low-power microcontrollers. By utilizing the 27$^{\text{th}}$ harmonic of square waves generated from Serial Peripheral Interface (SPI) and Inter-Integrated Circuit Sound (I2S) interfaces operating at 16 MHz, NoLoRa generates proper LoRa chirps. Commercial off-the-shelf (COTS) LoRa receivers at 433 MHz successfully decode these signals without requiring active RF components, such as power amplifiers, at the transmitter. The NoLoRa system achieves an average power consumption of 27 µA at a 1% duty cycle, demonstrating its suitability for battery-free operation via energy harvesting. Experimental validation confirms transmission ranges exceeding 100 m. The proposed system enables low-cost, long-range wireless communication for applications including remote environmental monitoring, asset tracking in logistics, and smart agriculture sensor networks.**

***Index Terms*—chirp spread spectrum (CSS), electromagnetic emissions, Internet of Things (IoT), long range (LoRa) modulation**

I. Introduction

The rapid proliferation of Internet of Things (IoT) devices has created demand for scalable, low-cost, and power-efficient communication solutions. Active radio technologies, such as Wi-Fi, ZigBee, and LoRa, provide reliable coverage [1] but suffer from high power consumption and deployment costs of several dollars per device. This limitation has driven research toward battery-free energy-harvesting systems that extract power from ambient sources, including solar, kinetic, or radio frequency (RF) energy [2], [3]. These systems enable maintenance-free operation in remote or resource-constrained environments. However, achieving long-range communication at microwatt power levels remains a fundamental challenge that existing technologies cannot address at scale.

The shift toward ultra-low-power operation has renewed interest in the electromagnetic behavior of digital systems. Electromagnetic (EM) emissions from microcontrollers (MCUs) and digital circuits, traditionally viewed as undesirable interference, are now being explored as potential communication channels. The widespread deployment of electronic equipment has simultaneously increased concerns about EM security. Unintentional EM radiation can inadvertently leak sensitive information. Military researchers recognized as early as the 1960s that computers emit exploitable electromagnetic radiation, later termed "compromising emanations" or "Tempest radiation" [4]. This discovery led to strict security protocols, including shielded enclosures and the "red/black" separation principle, to prevent information leakage. However, these efforts focused primarily on defense against unintentional emissions rather than their constructive application.

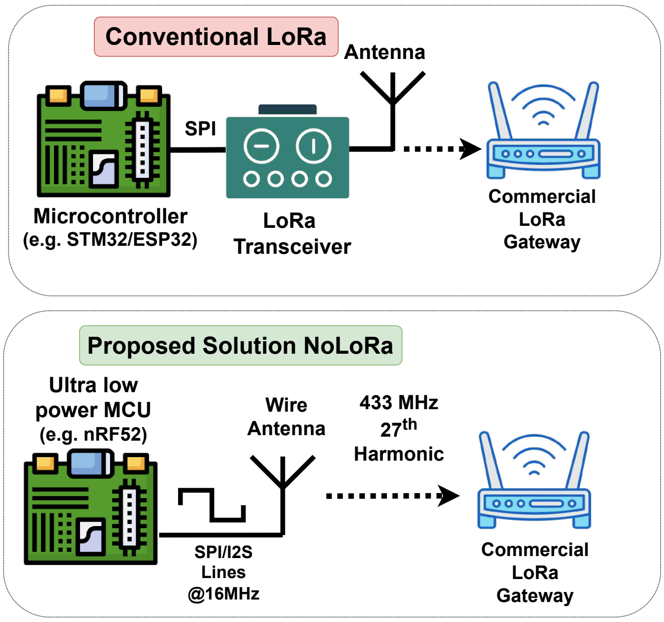

Fig. 1. Comparative architecture: traditional LoRa versus proposed NoLoRa design.

Recent research has demonstrated the potential of electromagnetic emanations for wireless communication. SideComm [5] utilizes processor-generated EM side-channels to enable low-overhead wireless communication in resource-constrained IoT devices without dedicated radio hardware. EMLoRa [6] exploits memory-based EM radiation combined with LoRa-like chirp spread spectrum modulation to create covert channels capable of penetrating severe shielding and achieving communication ranges exceeding several hundred meters. Noise-SDR [7] demonstrates random modulation of EM noise from unprivileged software, introducing new vectors for emission security analysis.

Complementing these active EM modulation approaches, passive backscatter communication has emerged as a promising paradigm for ultra-low-power wireless systems. In backscatter systems, devices reflect and modulate ambient RF signals rather than generating their own transmissions. Talla et al. [8] introduced LoRa Backscatter, the first wide-area backscatter system compatible with commercial LoRa hardware. The system achieves reliable communication up to 475 m between an RF source and receiver, extending to 2.8 km when the backscatter tag is co-located with the source. However, these systems require an active RF source, limiting truly independent battery-free operation. Ambient backscatter systems address this constraint by leveraging environmental RF signals.

Daskalakis et al. [9] presented LoRAB, a long-range ambient backscatter system that modulates chirp spread spectrum signals onto FM broadcasts. The system achieves a 130-m communication range with 103 nA front-end power consumption and a data rate of 88 bps. By exploiting ubiquitous FM signals, LoRAB eliminates the need for a dedicated transmitter, improving both stealth and power efficiency. However, performance depends critically on FM signal availability, limiting applicability in regions with poor broadcast coverage.

This work introduces NoLoRa, a novel system that achieves LoRa-compatible communication by exploiting natural electromagnetic emissions from MCU digital interfaces, eliminating the need for dedicated radio transceivers. Inspired by LoLRa [10], NoLoRa combines the ultra-low power characteristics of backscatter systems with independence from external RF sources. Section II details the NoLoRa chirp generation mechanism. Section III presents experimental results demonstrating power consumption and communication range. The paper concludes with a discussion of findings and future research directions.

II. Implementation Overview

A. LoRa Modulation and Chirp Characteristics

LoRa modulation was selected for this work due to its robustness against noise and multipath interference, long-range communication capability, and compatibility with commercial LoRaWAN gateways [6]. LoRa employs Chirp Spread Spectrum (CSS) modulation, where data is encoded through frequency-modulated chirps that sweep linearly across a defined bandwidth. Data symbols are represented by discrete frequency offsets within each chirp. The spreading factor (SF) parameter enables a trade-off between data rate and noise sensitivity, with higher SF values providing greater range at the cost of reduced throughput.

Fig. 2. Structure of a LoRa frame showing preamble, sync word, and payload chirps.

A LoRa upchirp is mathematically defined as

$$s(t) = A\cos\left(2\pi\left(f_c t + \frac{B}{2T}t^2\right)\right), \quad 0 \le t \le T \qquad (1)$$

where A is the amplitude, f_c is the carrier frequency, B is the bandwidth, and T is the symbol duration. The instantaneous frequency sweeps linearly from $f_c - B/2$ to $f_c + B/2$. A downchirp reverses this frequency sweep direction. Each LoRa frame comprises preambles (repeated upchirps), synchronization words, headers, payload symbols, and cyclic redundancy check (CRC) bits, as illustrated in Fig. 2. The predetermined frequency transitions of these chirps enable accurate coherent demodulation at the receiver.

B. Harmonics of a Square Wave and Energy Distribution

NoLoRa is able to take advantage of the ability to naturally radiate harmonics of digital lines like Serial Peripheral Interface (SPI) or Inter-Integrated Circuit Sound (I2S), to generate detectable LoRa-compatible signals. A square wave contains a wide harmonic series, composed of only the odd harmonics of its fundamental frequency. The Fourier series expansion of an ideal unit amplitude square wave with frequency f is given by

$$x(t) = \frac{4}{\pi}\sum_{n=1,3,5,\ldots}^{\infty}\frac{1}{n}\sin(2\pi n f_0 t) \qquad (2)$$

The Equation 2 consists of a sum of several sine waves. Each sine wave has a diminishing amplitude of $\frac{4}{\pi n}$ and only odd harmonics are present (like $n = 1, 3, 5, \ldots$). The frequency of each sine wave is nf_0 and together make a square wave with the fundamental frequency of f_0.

As a result, the amount of energy in each harmonic decreases as $1/n^2$. However, the higher-order harmonics still possess enough amplitude to allow emissions to be detected. In the case of NoLoRa, the 27^{th} harmonic of a 16 MHz square wave has a frequency of 432 MHz, which is conveniently found near the 433 MHz industrial, scientific, and medical (ISM EU433 [11]) band used by LoRa.

C. Software-Based Chirp Generation

LoRa chirps are generated digitally using precomputed upchirp and downchirp baseband samples stored in memory. The nRF52833 MCU from Nordic Semiconductor was selected as the main processing unit due to its ultra-low power sleep mode, consuming less than 1 µA. The MCU operates its SPI or I2S interface at 16 MHz. The resulting digital stream produces a 27th harmonic at −95 dBm. Although this power level is extremely low, it remains detectable by commercial LoRa receivers with noise floors approaching −130 dBm. Frequency shifting for each LoRa symbol is achieved through Direct Memory Access (DMA) memory pointer offsets, which select the appropriate chirp waveform segment for transmission. This approach eliminates real-time waveform generation by the Central Processing Unit (CPU), enabling continuous symbol streaming without processor intervention. DMA double buffering maintains ultra-low power consumption throughout operation.

Algorithm 1 Software implementation of NoLoRa.

```
One-time Initialization:
Generate_UpChirp();
Generate_DownChirp();
Store_Chirps_in_Memory();
Main Runtime Loop:
while true do
    Enter_DeepSleep_With_Memory_Retention();
    Wait_For_RTC_Wakeup();
    SensorData ← Read_Sensors();
    EncodedData ← LoRa_Encode(SensorData);   ▷ Error coding, header, CRC
    SymbolList ← Map_To_LoRa_Symbols(EncodedData);
    Configure_DMA(SymbolList);
    DMA_Start_Transfer_To_SPI_I2S();   ▷ Double buffering
    Enter_DeepSleep();   ▷ CPU sleeps during DMA transmission
end while
DMA Interrupt Handler:
procedure ON_DMA_SYMBOL_SHIFT
    Update_Memory_Pointer_For_Next_Symbol();
end procedure
```

Algorithm 1 illustrates the complete implementation. The architecture minimizes CPU activity by limiting processor wake events to periodic sensor reading and data packaging operations. High-speed waveform generation is handled exclusively by DMA transfers to the SPI/I2S peripheral, enabling continuous generation of LoRa-compatible chirps with minimal energy consumption.

III. Power Consumption and Results

The power consumption of the NoLoRa prototype was characterized across multiple LoRa configurations. Worldwide LoRaWAN regulations for end devices mandate a typical duty cycle of 1%, ensuring compliance with European Commission harmonization requirements for short-range device (SRD) radio spectrum usage [12]. NoLoRa achieves an average current consumption of 27 μA at 3 V, which remains effectively constant across all spreading factors. This ultra-low power consumption aligns with the system's intended application in energy-harvested and battery-free deployments.

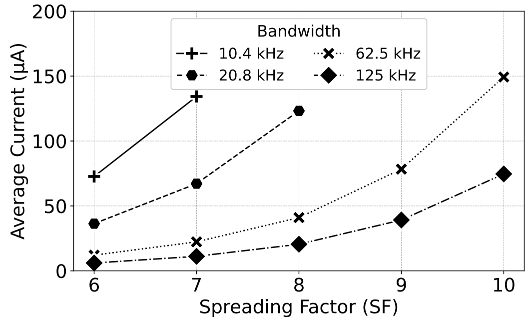

Fig. 3. Power consumption measurements of NoLoRa for a 4-byte packet with 8 preambles transmitted every 10 s, showing average current versus spreading factor for bandwidths of 10.4 kHz, 20.8 kHz, 62.5 kHz, and 125 kHz.

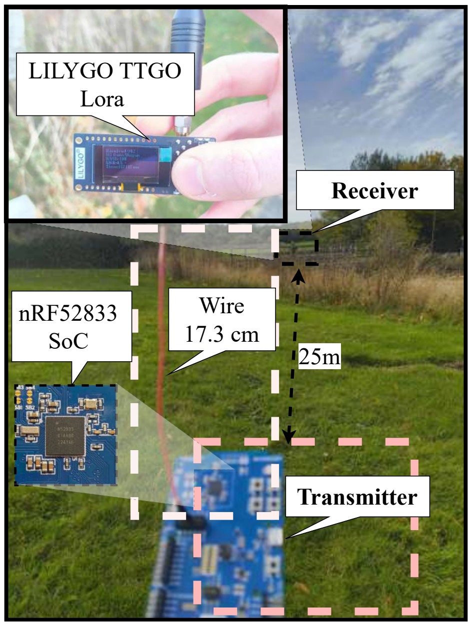

Fig. 4. Field testing setup at Heriot-Watt University demonstrating the NoLoRa system with a LILYGO TTGO LoRa receiver and nRF52833 MCU transmitter, configured with spreading factor 10, coding rate 4/8, and 125 kHz bandwidth.

Power consumption measurements were conducted using 4-byte packets with 8 preamble symbols, transmitted every 10 s across various modulation parameters. Average current consumption was measured for different combinations of SF, bandwidth (BW), and coding rate (CR), with results presented in Fig. 3. Increasing bandwidth reduces power consumption due to the inverse relationship between chirp duration and bandwidth. Conversely, higher spreading factors increase power consumption as chirp duration scales with SF [13]. Despite these variations, power consumption remains within the same order of magnitude across all configurations, demonstrating NoLoRa's compatibility with existing LoRa networks. Previous studies [14], [15] confirm that battery-free operation is achievable at these power levels, validating NoLoRa's potential for energy-harvested applications.

To verify the communication range of NoLoRa, field tests

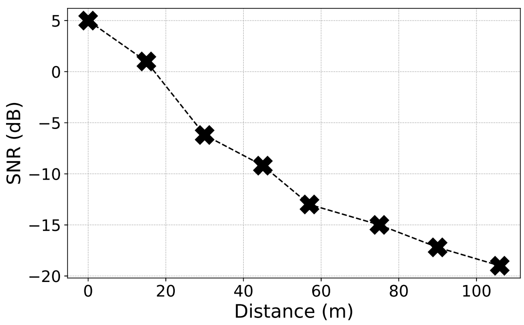

Fig. 5. Signal-to-noise ratio versus distance for the field test configuration.

were conducted in an open area with clear line-of-sight conditions. The test setup utilized a commercial LILYGO TTGO LoRa receiver as the gateway and the nRF52833 MCU as the NoLoRa transmitter (Fig. 4). Tests were performed with SF 10, CR $4/8$, BW 125 kHz, 10 preambles per packet, and carrier frequency 434 MHz to maximize communication range. LoRa-compatible packets were successfully recovered and demodulated at distances up to 110 m. At maximum range, the received signal strength indicator (RSSI) measured -121 dBm with a signal-to-noise ratio (SNR) of -19 dB. The SNR remained within demodulatable limits throughout all test conditions (Fig. 5), demonstrating that NoLoRa achieves medium-range, ultra-low-power communication without dedicated RF hardware, making it suitable for battery-free and large-scale IoT deployments.

IV. Conclusion and Future Work

This work introduces NoLoRa, a proof-of-concept system capable of transmitting LoRa-compatible signals without dedicated RF transceivers. By exploiting the 27^{th} harmonic of digital interfaces (SPI/I2S) on a low-power nRF52833 MCU, the system achieves communication ranges up to 110 m with an average power consumption of 27 μA at 3 V with a 1% duty cycle. These results demonstrate significant promise for battery-free IoT applications.

A custom printed circuit board (PCB) is under development, incorporating integrated power-harvesting circuits and optimized component placement to minimize parasitic losses and reduce power consumption compared to the current development board. The new design will include impedance-matching networks to enhance SNR, addressing the limitations of the existing prototype caused by the long, non-optimized trace connecting the GPIO pin to the MCU. While the current prototype (Fig. 4) radiates through a quarter-wave wire antenna (17.3 cm) without impedance matching, the final design will feature an SMA connector for proper antenna coupling.

The prototype generates harmonic emissions, requiring compliance with electromagnetic compatibility (EMC) regulations [16] for commercial deployment. Initial analysis indicates that emissions (-95 dBm at the 27^{th} harmonic) fall below levels considered problematic for commercial operation or interference. However, EMC compliance may necessitate additional filtering or attenuation. Future work includes testing the revised PCB in controlled environments and implementing energy-harvesting capabilities for the intended application scenarios.

References

[1] I. Cheikh, S. Roy, E. Sabir, and R. Aouami, "Energy, scalability, data and security in massive iot: Current landscape and future directions," *arXiv preprint arXiv:2505.03036*, May. 2025.

[2] S. D. Assimonis, S. N. Daskalakis, and A. Bletsas, "Sensitive and efficient RF harvesting supply for batteryless backscatter sensor networks," *IEEE Trans. Microw. Theory Techn.*, vol. 64, no. 4, pp. 1327–1338, Apr. 2016.

[3] K. Niotaki, F. Giuppi, A. Georgiadis, and A. Collado, "Solar/EM energy harvester for autonomous operation of a monitoring sensor platform," *Wireless Power Transfer*, vol. 1, no. 01, pp. 44–50, Mar. 2014.

[4] M. G. Kuhn and R. J. Anderson, "Soft tempest: Hidden data transmission using electromagnetic emanations," in *Information Hiding*, D. Aucsmith, Ed., Berlin, Heidelberg, 1998, pp. 124–142.

[5] J. Feng, T. Jacques, O. Abari, and N. Sehatbakhsh, "Everything has its bad side and good side: Turning processors to low overhead radios using side-channels," in *Proceedings of the 22nd International Conference on Information Processing in Sensor Networks (IPSN '23)*. New York, NY, USA: Association for Computing Machinery, 2023, pp. 288–301.

[6] C. Shen, T. Liu, J. Huang, and R. Tan, "When LoRa Meets EMR: Electromagnetic Covert Channels Can Be Super Resilient," in *2021 IEEE Symposium on Security and Privacy (SP)*, 2021, pp. 1304–1317.

[7] G. Camurati and A. Francillon, "Noise-SDR: Arbitrary Modulation of Electromagnetic Noise from Unprivileged Software and Its Impact on Emission Security," in *2022 IEEE Symposium on Security and Privacy (SP)*, 2022, pp. 1193–1210.

[8] V. Talla, M. Hessar, B. Kellogg, A. Najafi, J. R. Smith, and S. Gollakota, "LoRa backscatter: Enabling the vision of ubiquitous connectivity," in *Proc. ACM Int. joint Conf. on Pervasive and Ubiq. Comp.*, Orlando, Florida, USA, Sep. 2017.

[9] S. N. Daskalakis, A. Georgiadis, M. M. Tentzeris, G. Goussetis, and G. Deligeorgis, "The new era of long-range "zero-interception" ambient backscattering systems: 130 m with 130 na front-end consumption," *MDPI Sensors*, vol. 22, no. 11, May 2022.

[10] C. Lohr, "LoLRa: Transmit LoRa Frames Without a Radio," https://github.com/cnlohr/lolra, 2025, accessed: 2025-10-12.

[11] LoRa Alliance Technical Committee, "LoRaWAN™ Regional Parameters Version 1.0," LoRa Alliance, Inc., Tech. Rep. V1.0, Jul. 2016, companion to LoRaWAN Specification 1.0.2.

[12] E. Commission, "Commission implementing decision (eu) 2019/1345 of 2 august 2019 amending decision 2006/771/ec updating harmonised technical conditions in the area of radio spectrum use for short-range devices (oj l 212, 13.8.2019)," *Official Journal of the European Union*, May. 2019.

[13] A. Augustin, J. Yi, T. Clausen, and W. M. Townsley, "A study of lora: Long range & low power networks for the internet of things," *MDPI Sensors*, vol. 16, no. 9, Sep. 2016.

[14] S. N. Daskalakis, R. Correia, G. Goussetis, M. M. Tentzeris, N. B. Carvalho, and A. Georgiadis, "Four-pam modulation of ambient fm backscattering for spectrally efficient low-power applications," *IEEE Trans. Microw. Theory Techn.*, vol. 66, no. 12, pp. 5909–5921, Dec. 2018.

[15] S. N. Daskalakis, G. Goussetis, S. D. Assimonis, M. M. Tentzeris, and A. Georgiadis, "A uW backscatter-morse-leaf sensor for low-power agricultural wireless sensor networks," *IEEE Sensors J.*, vol. 18, no. 19, pp. 7889–7898, Oct. 2018.

[16] *Industrial, Scientific and Medical Equipment — Radio-frequency Disturbance Characteristics — Limits and Methods of Measurement*, CENELEC / IEC / CISPR Std. EN 55 011:2016/A2:2021, 2021.